Supporting Information for:

Accessing Ni(III)-Thiolate versus Ni(II)-Thiyl Bonding in a Family of Ni-N_2S_2 Synthetic Models of NiSOD

Ellen P. Broering,[†] Stephanie Dillon,[‡] Eric M. Gale, [†] Ramsey A. Steiner, [†] Joshua Telser, [§] Thomas C. Brunold, [‡] and Todd C. Harrop[*,†]

[†]Department of Chemistry and Center for Metalloenzyme Studies, The University of Georgia, 1001 Cedar Street, Athens, Georgia 30602, United States

[‡]Department of Chemistry, University of Wisconsin, Madison, Wisconsin 53706, United States

[§]Department of Biological, Chemical and Physical Sciences, Roosevelt University, 430 South Michigan Avenue, Chicago, Illinois 60605, United States

*E-mail: tharrop@uga.edu

Table of Contents:

Table S1. Summary of crystal data and intensity collection and structure refinement parameters for $[Ni_4(nmp)_4]$ (**1**), $(Et_4N)[Ni(nmp)(SPh\text{-}o\text{-}NH_2)]$ (**2**), and $(Et_4N)[Ni(nmp)(SPh\text{-}p\text{-}NH_2)]$ (**4**).

Parameters	**1**	**2**	**4**
Formula	$C_{32}H_{32}N_8Ni_4O_4S_4$	$C_{22}H_{34}N_4NiOS_2$	$C_{22}H_{34}N_4NiOS_2$
Formula weight	955.70	493.36	493.36
Crystal system	Monoclinic	Monoclinic	Monoclinic
Space group	C2/c	*P*2(1)/n	*P* 21/c
Crystal color, habit	Red	Red, blade	Red, blade
a, Å	19.4038(19)	11.5155(19)	20.0499(11)
b, Å	13.7950(14)	10.0686(16)	11.8010(7)
c, Å	15.5713(16)	20.095(3)	20.4272(13)
α, deg	90	90	90
β, deg	126.8520(10)	92.038(2)	100.585(1)
γ, deg	90	90	90
V, $Å^3$	3335.2(6)	2328.4(7)	4751.0(5)
Z	4	4	8
$\rho_{calcd,}$ g/cm^3	1.903	1.407	1.379
T, K	100(2)	100(2)	100(2)
abs coeff, μ (MoKα), mm^{-1}	2.528	1.034	1.014
θ limits, deg	1.97-25.99	2.01-30.03	2.002-30.519
total no. of data	19261	34465	75036
no. of unique data	3274	6815	14491
no. of parameters	263	271	541
GOF of F^2	1.080	1.023	1.021
R_1,[a] %	0.0393	0.0378	0.0371
wR_2,[b] %	0.1031	0.0873	0.0959
max, min peaks, $e/Å^3$	0.9280, 0.7029	0.420, -0.497	0.696, -0.651

[a] $R_1 = \Sigma| |F_O| - |F_c| | / \Sigma |F_O|$; [b] $wR_2 = \{\Sigma[w(F_o^2 - F_c^2)^2]/\Sigma[w(F_o^2)^2]\}^{1/2}$

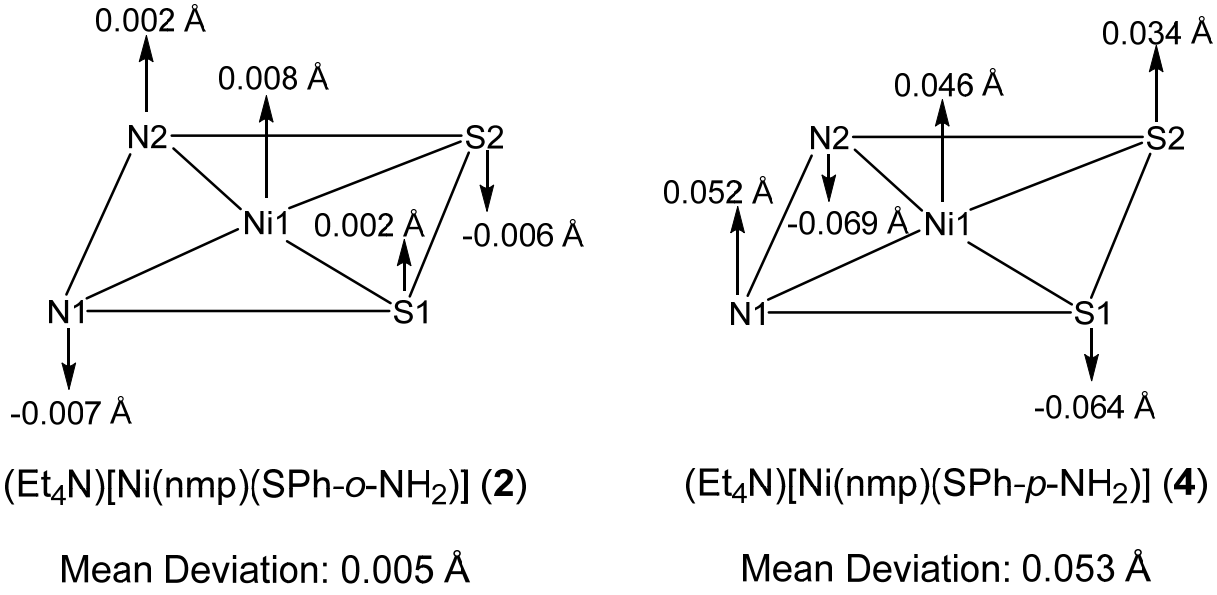

$(Et_4N)[Ni(nmp)(SPh\text{-}o\text{-}NH_2)]$ (**2**)

Mean Deviation: 0.005 Å

$(Et_4N)[Ni(nmp)(SPh\text{-}p\text{-}NH_2)]$ (**4**)

Mean Deviation: 0.053 Å

Figure S1. Schematic representation of the NiN_2S_2 plane for $(Et_4N)[Ni(nmp)(SPh\text{-}o\text{-}NH_2)]$ (**2**) and $(Et_4N)[Ni(nmp)(SPh\text{-}p\text{-}NH_2)]$ (**4**) and deviations of each atom from the weighted least-square plane. N2, N1, and S1 represent the donor atoms derived from the nmp^{2-} ligand, whereas S2 originates from the exogenous S donor (S_{exo}).

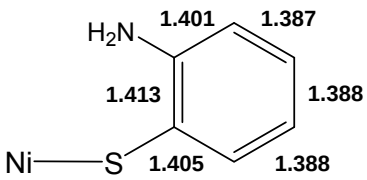

(**2**)

C-S: 1.7730 Å
C-N: 1.392 Å
C-C (avg.): 1.397 ± 0.011 Å

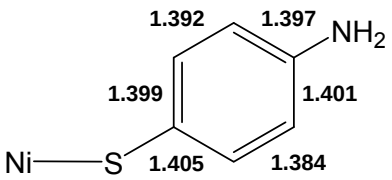

(**4**)

C-S: 1.7722 Å
C-N: 1.406 Å
C-C (avg.): 1.396 ± 0.007 Å

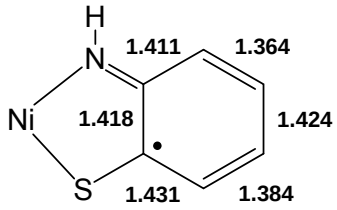

Ni-coordinated o-iminothiosemiquinonate
C-S: 1.724 Å
C-N: 1.348 Å
C-C (avg.): 1.405 ± 0.026 Å

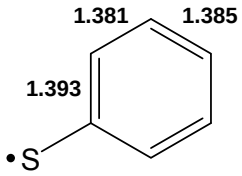

phenylthiyl radical (calc.)
C-S: 1.750 Å
C-C (avg.): 1.386 ± 0.006 Å

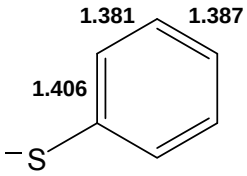

phenylthiolate anion (calc.)
C-S: 1.756 Å
C-C (avg.): 1.391 ± 0.013 Å

Chart S1. *Top*: Relevant bond distances of the S_{exo} ligand in the anions of **2** and **4**. *Bottom*: Same parameters for a structurally-characterized Ni(II)-N,S-coordinated *o*-iminothiosemiquinonate (see *J. Am. Chem. Soc.* **2001**, *123*, 10012) and the calculated bond lengths of the phenylthiyl radical and phenylthiolate anion (ROHF/3-21G*, see *J. Phys. Chem.* **1992**, *96*, 5344).

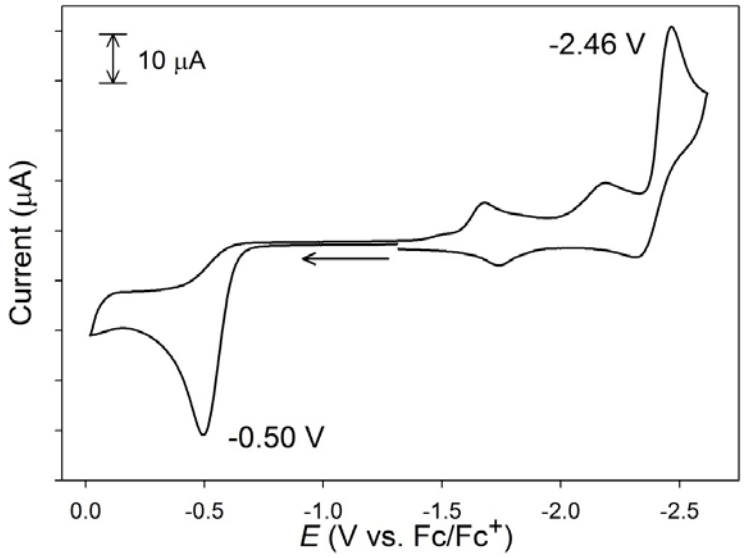

Figure S2. CV of an 8 mM solution of **4** in DMF at RT (glassy carbon working electrode, 0.1 M $^{n}Bu_4NPF_6$ as supporting electrolyte, 100 mV/s scan speed). Arrow shows direction of scan.

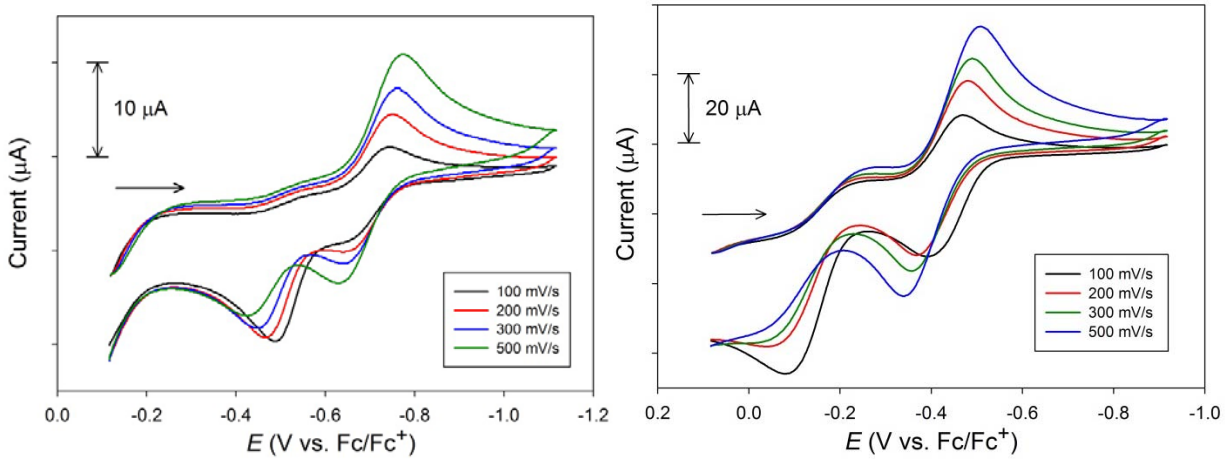

Figure S3. CV of 8 mM solutions of **2** (left) and **3** (right) in DMF at RT (glassy carbon working electrode, 0.1 M $^{n}Bu_4NPF_6$ as supporting electrolyte, 100 mV/s scan speed). Arrow shows the direction of the scan.

Table S2. EPR parameters for Ni(III) coordination complexes with N_xS_y donor sets relevant to the present study.

Complex	*g* values: [max, mid, min], avg	Ground state assignment [a]	Reference
***cis*-N2S2 donor set, N3S2 donor set [b]**			
[Ni(nmp)(SPh-*o*-NH_2-*p*-CF_3)] (**3^{ox}**)	[2.132, 2.028, 2.004], 2.055	$\left(d_{z^2}^{\ 1}\right)$	this work
$[Ni(emb)]^-$	[2.29, 2.11, 2.04], 2.15	uncertain	*Inorg. Chem.* **1987**, *26*, 3645.
$[Ni(ema)]^-$	[2.23, 2.18, 2.01], 2.14	$d_{z^2}^{\ 1}$	*Inorg. Chem.* **1991**, *30*, 734.
$[Ni(phma)]^-$	[2.20, 2.17, 2.01], 2.13	$d_{z^2}^{\ 1}$	*Inorg. Chem.* **1991**, *30*, 734.
$[Ni(emi)]^-$	[2.44, 2.27, 1.96], 2.22	uncertain	*Inorg. Chem.* **1991**, *30*, 734.
$[Ni(phmi)]^-$ $[Ni(phmi)(py)]^-$	[2.55, 2.14, 2.00], 2.23 [2.313, 2.281, 2.000], 2.198	uncertain $d_{z^2}^{\ 1}$	*Angew. Chem. Int. Ed.* **1998**, *37*, 260
$[Ni(ema)\cdot(CH_2)_3]^-$	[2.36, 2.23, 2.01], 2.20	$d_{z^2}^{\ 1}$	*Inorg. Chem.* **2007**, *46*, 7536.
$[Ni(L_1)]$	[2.26, 2.19, 2.01], 2.15	$d_{z^2}^{\ 1}$	*Inorg. Chem.* **2014**, *53*, 6512.
$[Ni(L)(im)]^{+}$ [c]	[2.315, 2.177, 2.029], 2.174	$d_{z^2}^{\ 1}$	*Inorg. Chem.* **2010**, *49*, 6399.
S4 donor set [d]			
$[Ni(nbdt)_2]^-$	[2.14, 2.05, 2.05], 2.08	uncertain	*J. Am. Chem. Soc.* **1990**, *112*, 3218.
$[Ni(mnt)_2]^-$	[2.14, 2.04, 1.99], 2.06	$\left(d_{xz}^{\ 1}\right)$ [g]	*Inorg. Chem.* **1998**, *37*, 1361.
$[Ni(S_2C_2Me_2)_2]^-$	[2.118, 2.041, 2.000], 2.053	$\left(d_{xz}^{\ 1}\right)$ [g]	*Inorg. Chem.* **2001**, *40*, 4257.
$[Ni(S(NH)C_6H_4)_2]^-$	[2.126, 2.028, 2.005], 2.053	uncertain	*J. Am. Chem. Soc.* **1967**, *89*, 2866.
***trans*-N2S4 donor set**			
$[Ni(pdtc)_2]^-$ [e]	[2.137, 2.137, 2.038], 2.104	$d_{z^2}^{\ 1}$	*J. Am. Chem. Soc.* **1990**, *112*, 2955.
N6 donor set [f]			
$[Ni(H\__3G_3a)(NH_3)_2]$	[2.178, 2.178, 2.019], 2.125	$d_{z^2}^{\ 1}$	*Inorg. Chem.* **1978**, *17*, 1630.
$[Ni(Me_2[14]aneN_4)(NCO)_2]^+$	[2.169, 2.169, 2.055], 2.131	$d_{z^2}^{\ 1}$	*Inorg. Chem.* **1973**, *12*, 1.

Ligand abbreviations: ema = *N*,*N*′-ethylenebis-2-mercaptoacetamide; (ema)·$(CH_2)_3$ = *N*,*N*′-ethylenebis(2-propylmercaptoacetamide); emb = *N*,*N*′-ethylenebis(*o*-mercaptobenzamide); emi = *N*,*N*′-ethylenebis-2-mercaptoisobutyramide; H_$_3$G$_3$a = trianion (i.e., mono-H) of tripeptide glycylglycylglycinamide; im = imidazole; L = dianion of 2,2′-(2,2′-bipyridine-6,6′-diyl)bis(1,1-diphenylethanethiol); L_1 = trianion of *N*-(2-mercapto-2-methylpropanoyl)-*N*′-(2-mercapto-2-methylpropyl)-1,2-diaminoethane; Me_2[14]aneN_4 = 2,3-dimethyl-1,4,8,11-tetraazacyclotetradecane; mnt = dianion of maleonitriledithiolate ($S_2C_2(CN)_2^{2-}$); nbdt = dianion of norbornane-2,3-dithiolate; nmp = dianion of *N*-(2-mercaptoethyl)picolinamide); pdtc = dianion of pyridine-2,6-bis(thiocarboxylate); phma = *N*,*N*′-1,2-phenylenebis-2-mercaptoacetamide); phmi = tetraanion of *N*,*N*′-1,2-phenylenebis(2-sulfanyl-2-methylpropionamide); py = pyridine; $S(NH)C_6H_4)_2^-$ = dianion of *o*-amidothiophenolate.

[a] As determined in the original work, parentheses indicates a ground state that is extensively delocalized onto the ligands, as opposed to being largely Ni-3*d*-centered. For a detailed discussion of $\mathbf{3^{ox}}$, see the main text.

[b] In a number of cases for these four-coordinate N2S2 donor set complexes, imine N donor base (typically pyridine or imidazole) was added which coordinates on one axial position and gives a characteristic triplet hyperfine splitting (^{14}N, I = 1) at g_{min}, indicating that this corresponds to the molecular z direction (i.e., so that this is g_z) and that the ground state is $d_{z^2}^1$; however, a shift in the ground state may have occurred with base binding (e.g., for pyridine binding to $[Ni(emi)]^-$). Such EPR results of axial base binding are not included here, except for the case of [Ni(phmi)]-, as a representative example, and the last member of this series, as explained in footnote *c*.

[c] For this complex, no formal Ni(III) species with an N2S2 donor set was observed. Upon oxidation of the four-coordinate Ni(II) parent compound, [Ni(L)] (S2N2 donor set), a diamagnetic di-Ni(III) complex is formed; however, addition of excess imidazole to this complex leads to formation of mononuclear $[Ni(L)(im)]^+$, which has a $d_{z^2}^1$ ground state as supported by extensive computational analysis (calculated spin density on Ni alone = 82%; calculated g = [2.252, 2.199, 2.071]).

[d] The electronic structure of such square-planar S4 donor set bis-dithiolato complexes has historically been the source of much controversy (see *Inorg. Chem.* **2011**, *50*, 9741; *Chem.-Eur. J.* **2007**, *13*, 2783). Among many examples, the dimethylthiolene complex listed herein has been thoroughly analyzed (see *Inorg. Chem.* **2001**, *40*, 4257; *Chem.-Eur. J.* **2003**, *125*, 9158). The electronic structure of the nbdt complex has not been so analyzed (and that its reported EPR is axial is unexpected), but may be similar to the mnt complex; the nbdt complex does not coordinate axial bases, in contrast to those with more unambiguous $d_{z^2}^1$ ground states (e.g., the (ema)·$(CH_2)_3$, emb, and emi complexes, and the pdtc complex with its "built-in" axial imino N-

donors). Its ground state was given as $\left(d_{x^2-y^2}{}^1\right)$, but this seems unreasonable in light of subsequent experimental and theoretical studies on such systems.

[e] This 6-coordinate complex has a *trans*-N2S4 donor set. Hyperfine coupling from two equivalent, axial ^{14}N ligands was well resolved at both $g_\perp$ and $g_\parallel$. A complex enriched in ^{61}Ni (I = 3/2) was also prepared and all evidence support a $d_{z^2}{}^1$ ground state.

[f] These 6-coordinate complexes with non-redox active ligands are classic examples of Ni(III) with $d_{z^2}{}^1$ ground state. The tripeptide complex has equivalent, *trans* ammine ligands which give rise to resolved ^{14}N hyperfine coupling at $g_\parallel$; the tetraaza macrocycle complex has equivalent, *trans N*-cyanato ligands; the EPR data is for powder, hence no hyperfine coupling was resolved.

[g] The coordinate system used by Huyett *et al*. for the mnt complex was defined so that the *z* axis was perpendicular to the molecular plane, and the *y* axis bisected the chelate rings with the *x* axis between the rings; the later model of Lim *et al*., which is used here, defined the *x* axis as bisecting the chelate ring and the *y* axis bisecting the S-Ni-S angle external to the chelates. In the more recent calculations, those for the dimethyldithiolene, the unpaired spin is only partially (25%; with 60% on the S atoms) on Ni (in $3d_{xz}$ AO; $5b_{2g}$ using D_{2h} symmetry) (see *J. Am. Chem. Soc.* **2003**, *125*, 9158). The calculated *g* values for this complex are: g = [2.115, 2.040, 1.969], in excellent agreement with experiment.

Chart S2. Workup flowchart for the reaction of $\mathbf{3^{ox}}$ with KO_2 in DMF at RT.

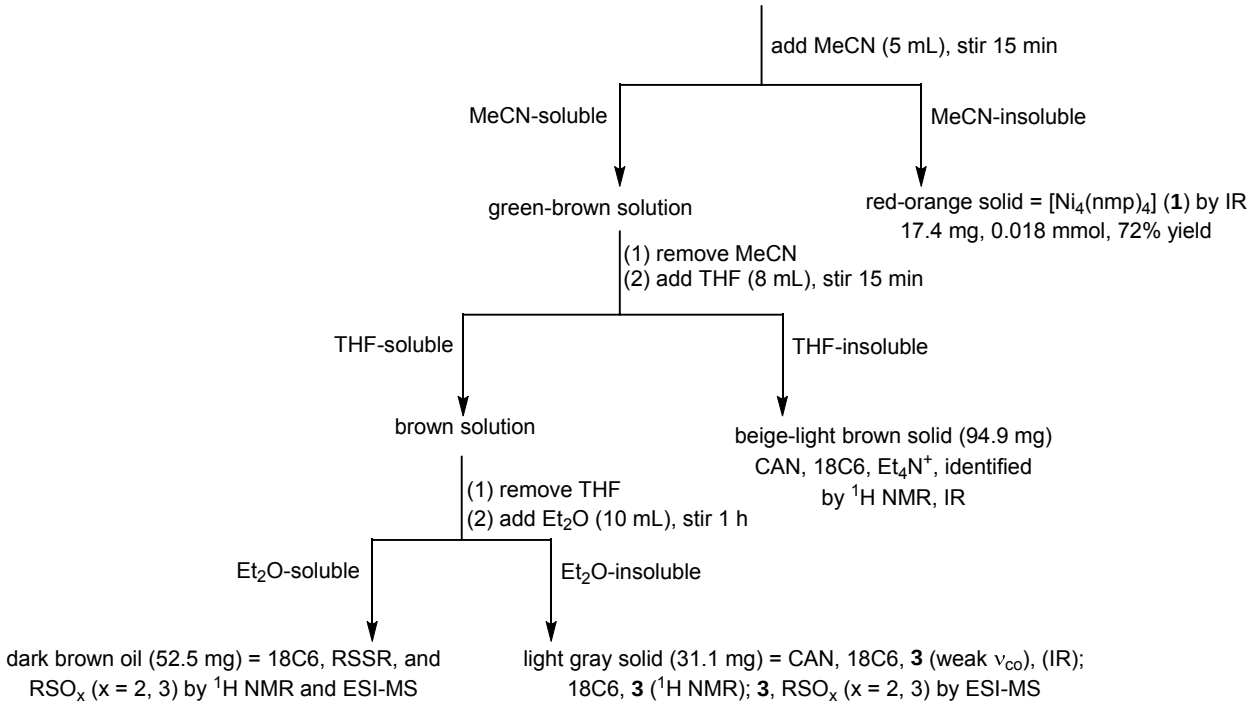

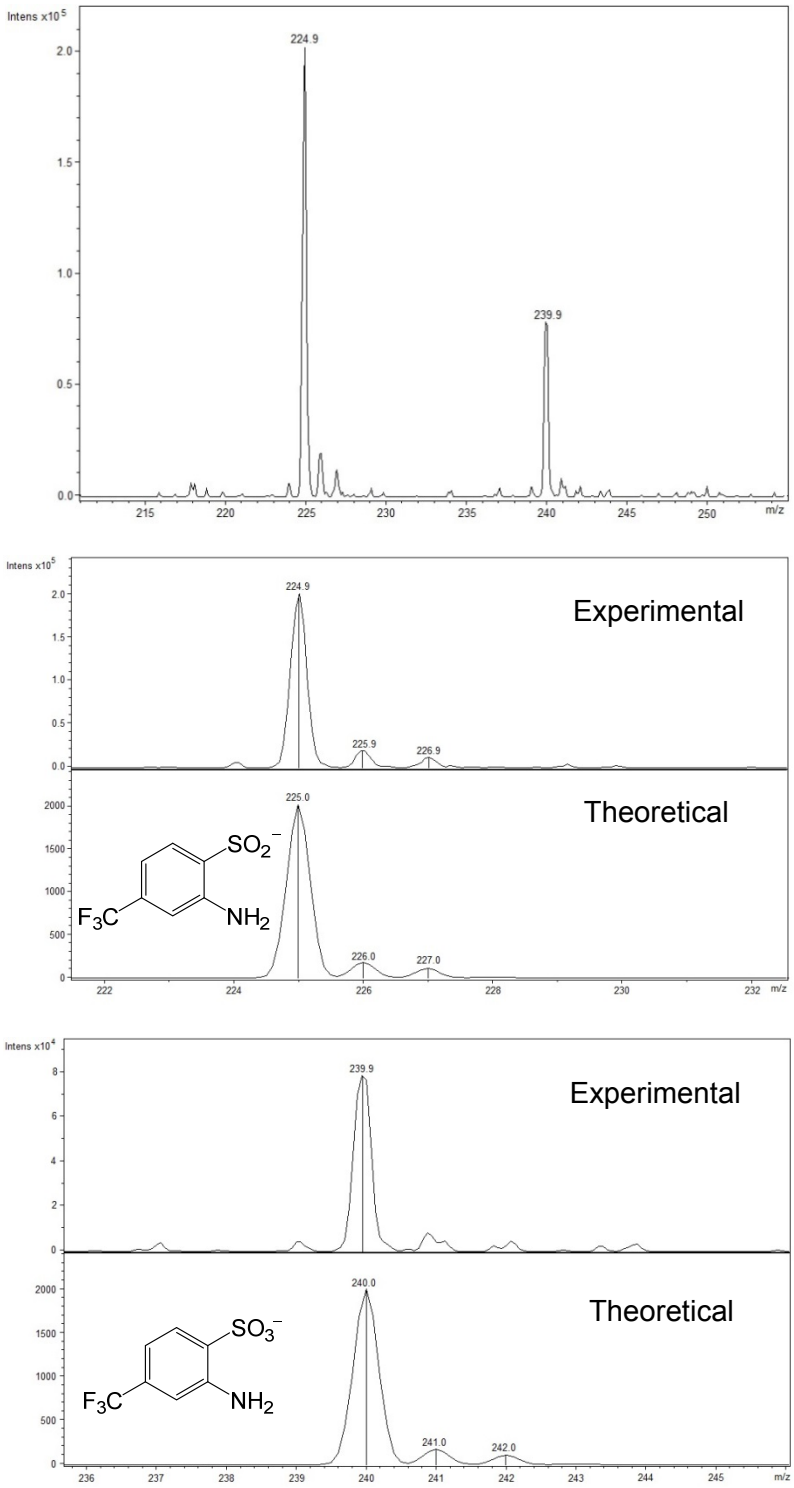

Figure S4. Low resolution ESI-MS (negative mode) of the Et_2O-soluble portion from Chart S2. Middle and bottom represent a zoom-in of the *m/z* 224.9 and 239.9 peaks. Theoretical fit on the bottom.

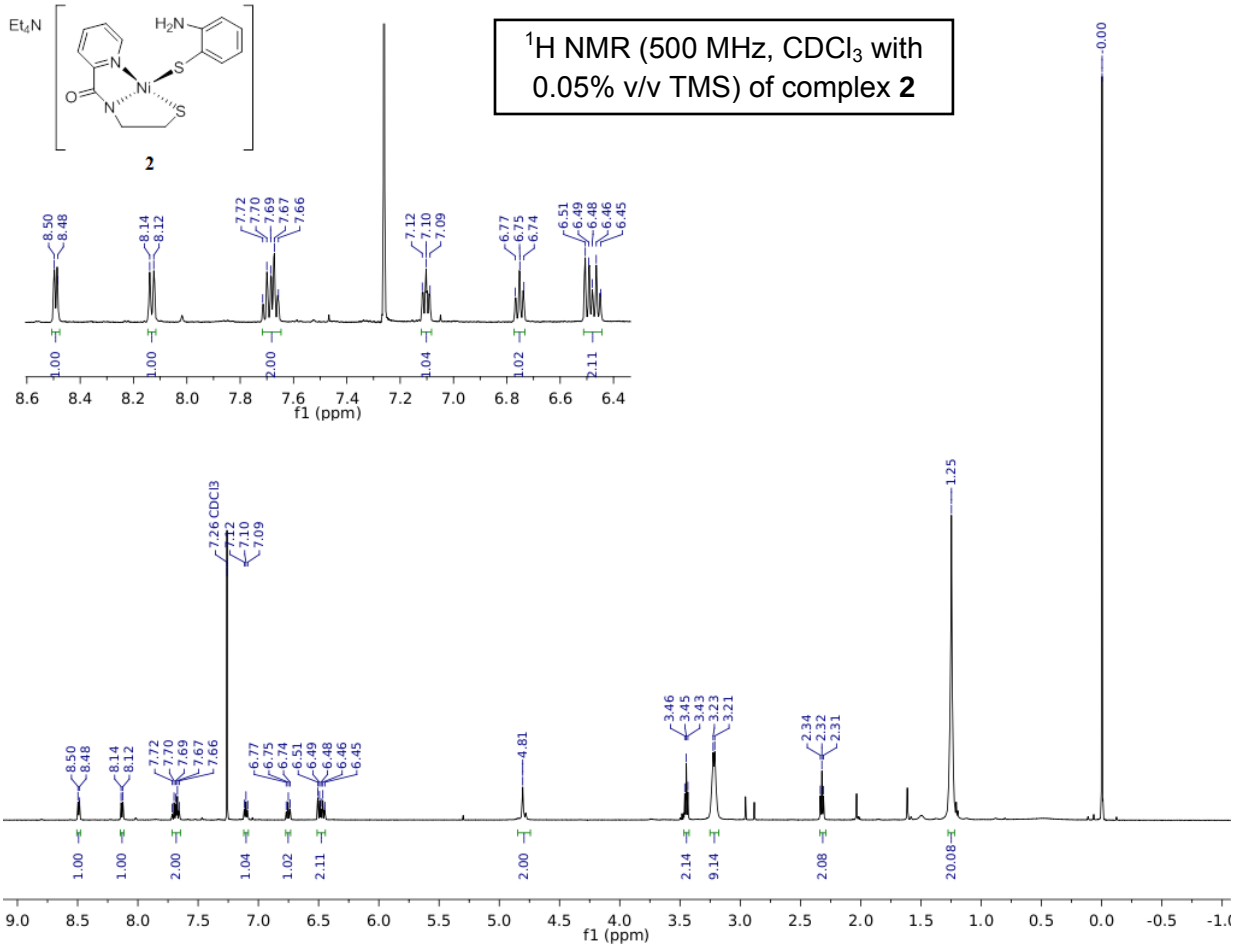

Figure S5. ^{1}H NMR spectrum of **2** in $CDCl_3$ containing 0.05% v/v TMS at RT. Inset shows expanded aromatic region. Residual protio solvent (7.26 ppm), H_2O (1.61 ppm), and TMS (0.00 ppm) are present. A minor amount of DMF (8.02, 2.96, 2.88 ppm) and MeCN (2.03 ppm) from workup are also present.

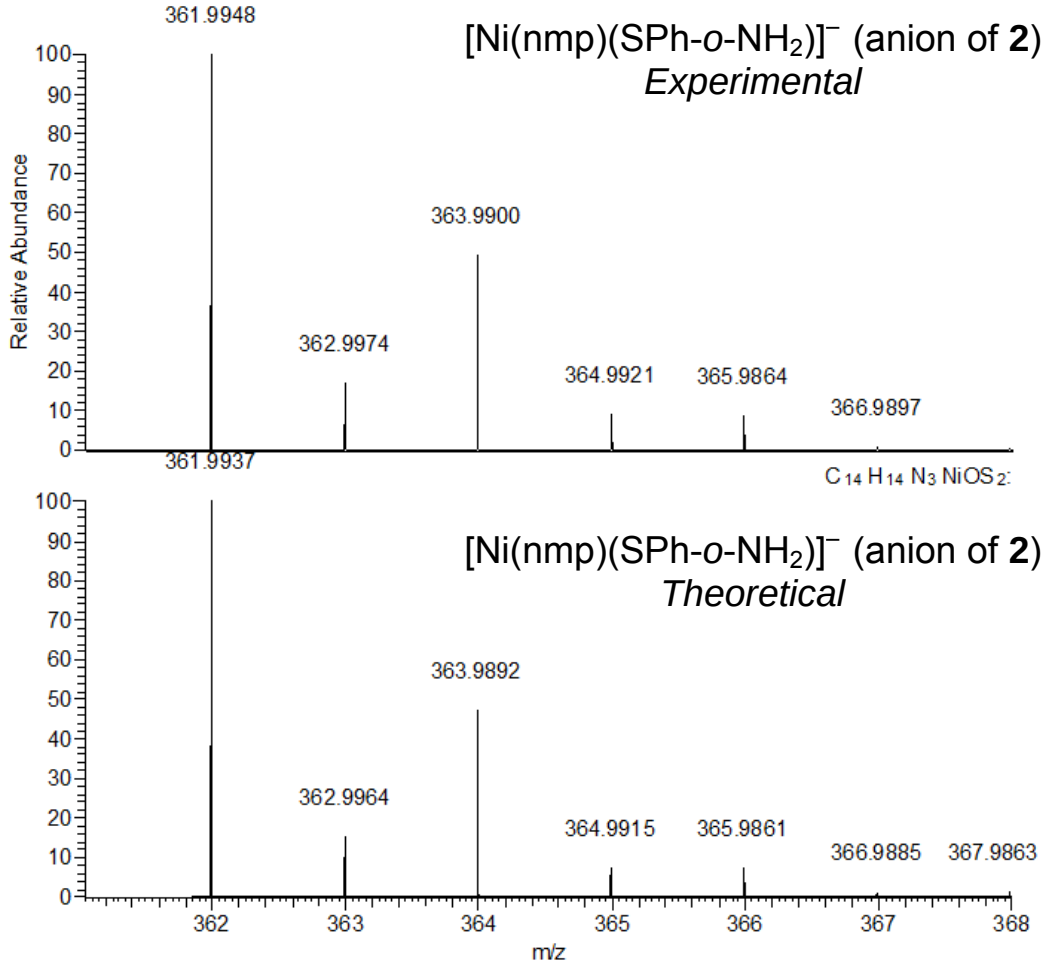

Figure S6. *Top*: High resolution ESI-MS (negative mode) of the anion of **2** $[M\text{-}Et_4N]^-$ in MeCN at RT. *Bottom*: Theoretical MS for the anion of **2**.

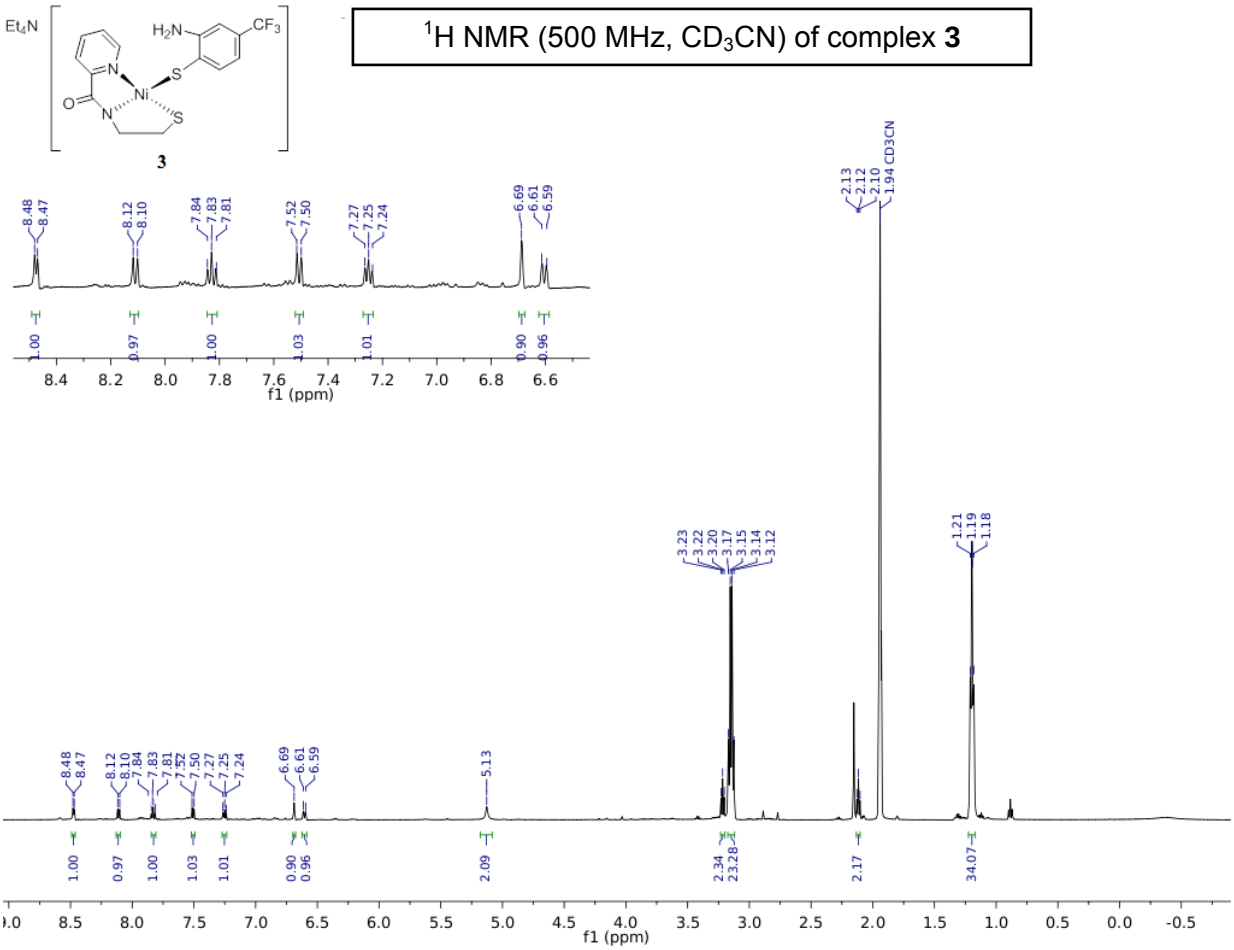

Figure S7. ^{1}H NMR spectrum of **3** in CD_3CN at RT. Inset shows expanded aromatic region. Residual protio solvent (1.94 ppm) and H_2O (2.13 ppm) are present. A minor amount of DMF (7.92, 2.89, 2.77 ppm) and Et_2O (3.42, 1.12 ppm) from workup are also present.

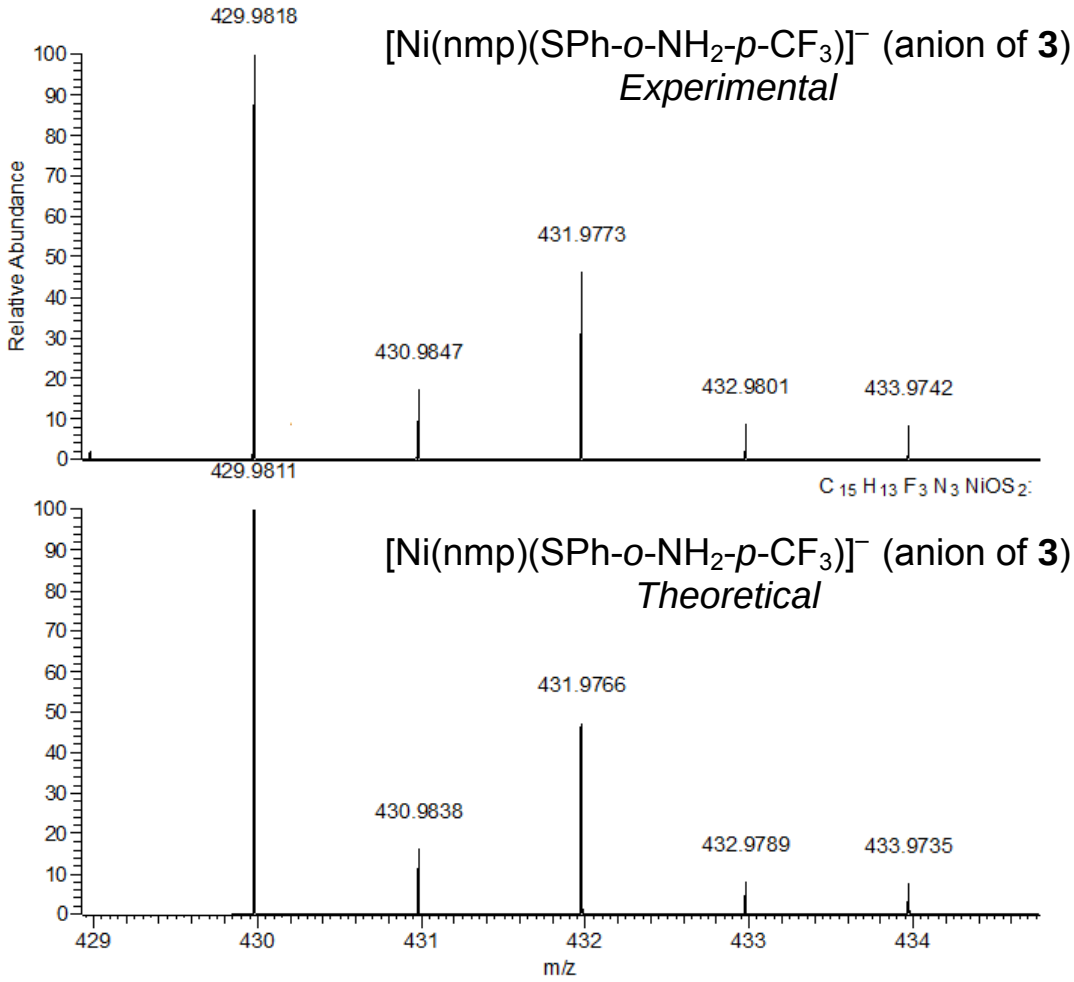

Figure S8. *Top*: High resolution ESI-MS of the anion of **3** $[M\text{-}Et_4N]^-$ in MeCN at RT. *Bottom*: Theoretical MS for the anion of **3**.

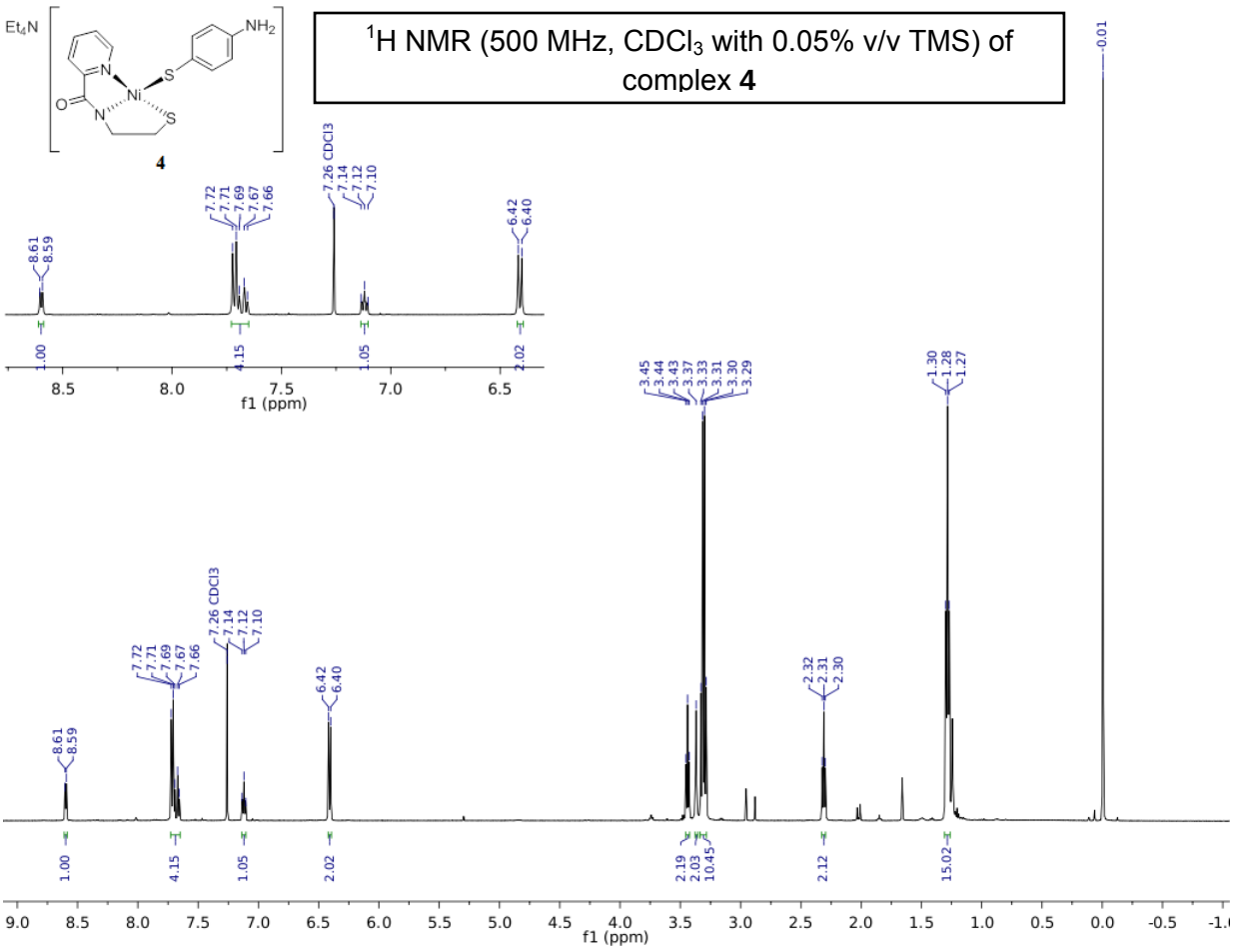

Figure S9. ^{1}H NMR spectrum of **4** in $CDCl_3$ containing 0.05% v/v TMS at RT. Inset shows expanded aromatic region. Residual protio solvent (7.26 ppm), H_2O (1.66 ppm), and TMS (0.00 ppm) are present. A minor amount of DMF (8.02, 2.95, 2.88 ppm), THF (3.74, 1.85 ppm), and MeCN (2.03 ppm) from workup are also present.

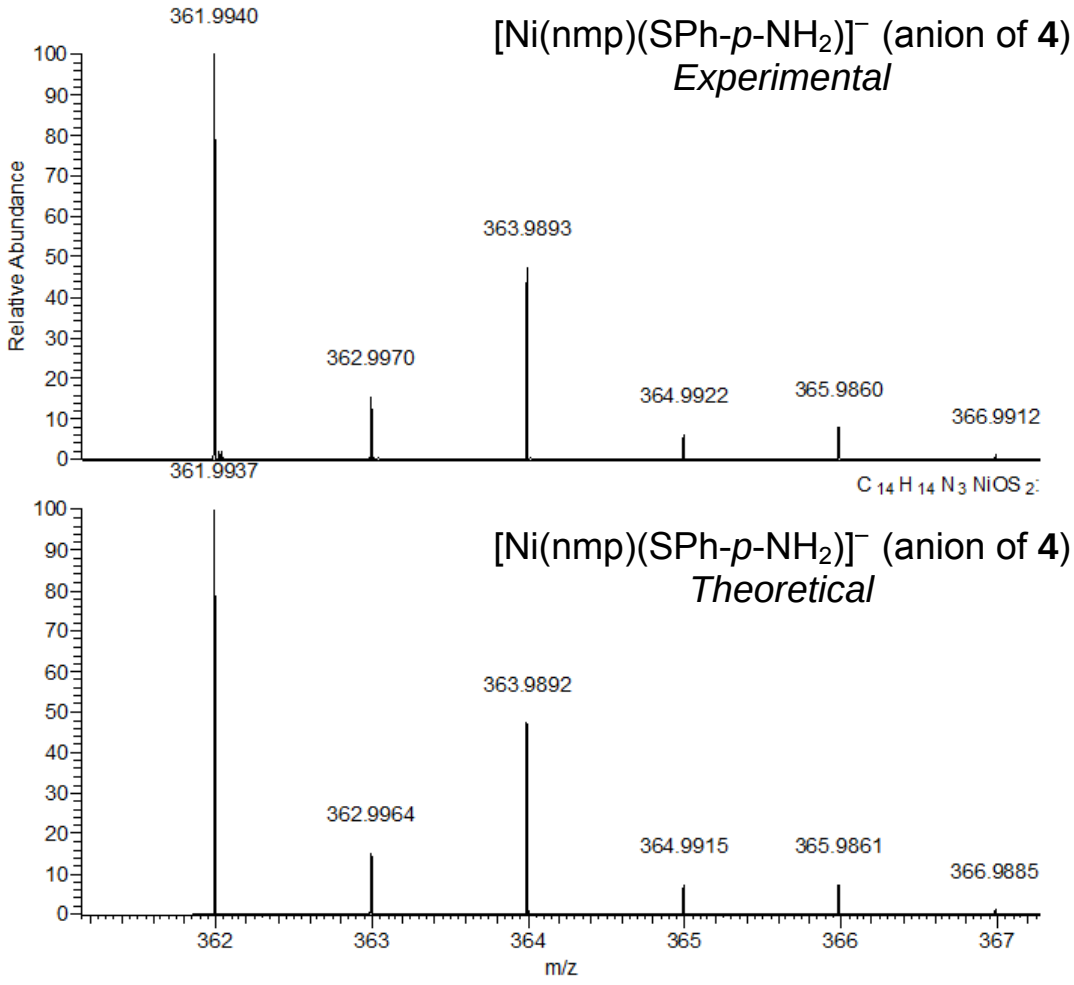

Figure S10. *Top*: High resolution ESI-MS of the anion of **4** [M-Et_4N]$^-$ in MeCN at RT. *Bottom*: Theoretical MS of the anion of **4**.

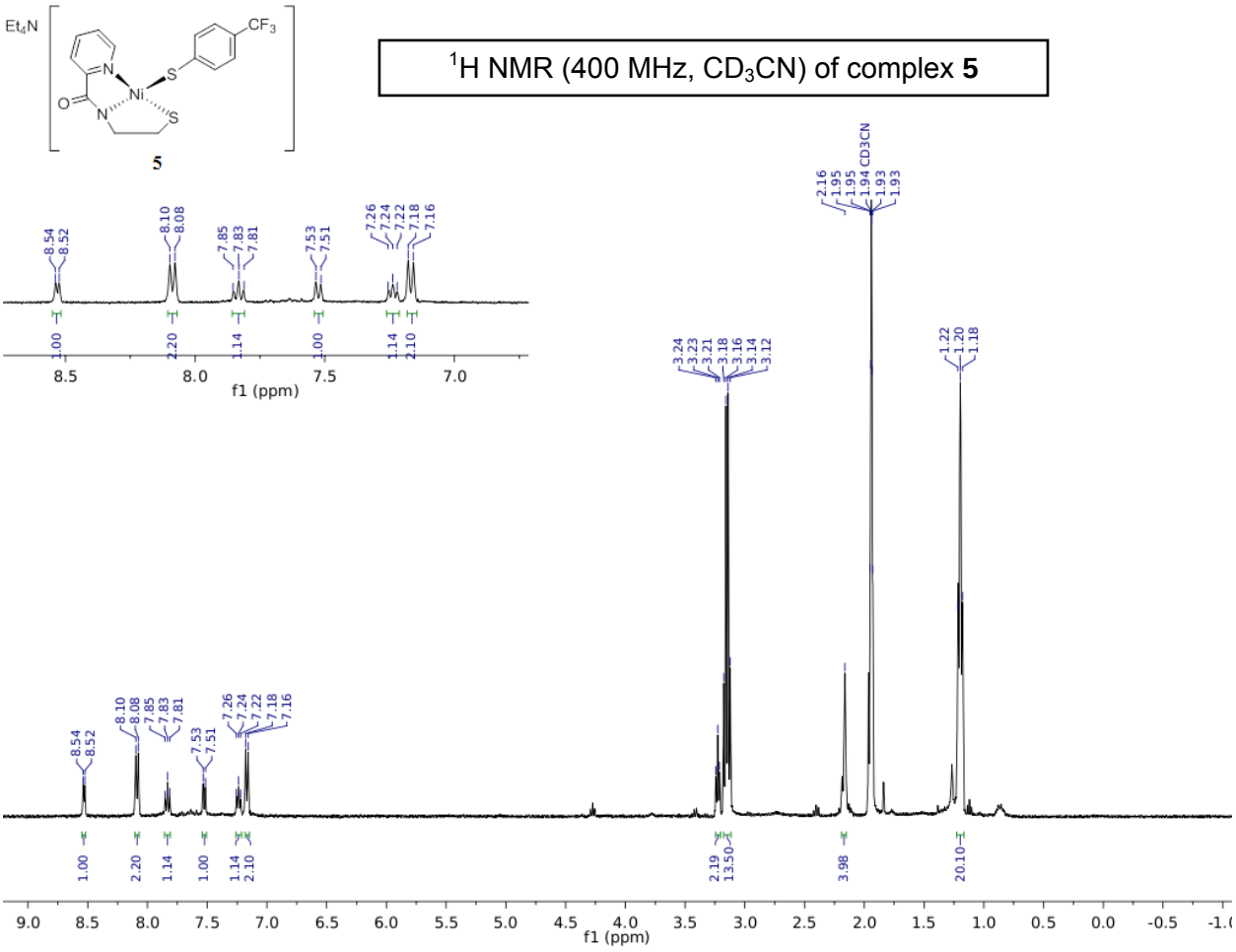

Figure S11. ^{1}H NMR spectrum of **5** in CD_3CN at RT. Inset shows expanded aromatic region. Residual protio solvent (1.94 ppm) and H_2O (2.16 ppm) are present. A minor amount of THF (3.64, 1.80 ppm) and Et_2O (3.42, 1.12 ppm) from workup is also present.

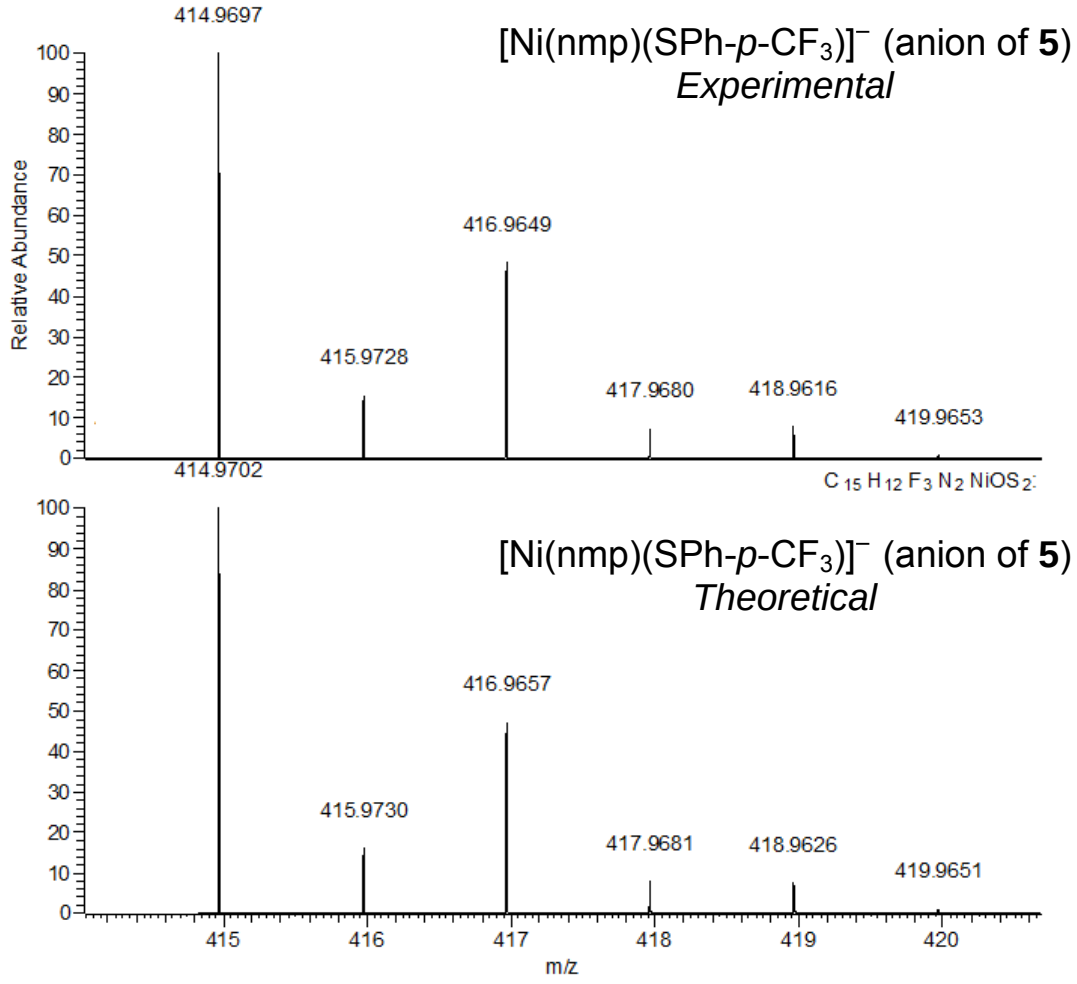

Figure S12. *Top*: High resolution ESI-MS of the anion of **5** $[M\text{-}Na]^-$ in MeCN at RT. *Bottom*: theoretical MS of the anion of **5**.